Proceeding Paper

Effects of Ni Content and Alloying Elements on Electrical Conductivity, Mechanical Properties, and Hot Tearing Susceptibility of Al-Ni-Based Alloys †

Farnaz Yavari [1],*, Ahmed Y. Algendy [1], Mousa Javidani [1], Lei Ray Pan [2] and X.-Grant Chen [1]

1   Department of Applied Science, University of Quebec at Chicoutimi, Saguenay, QC G7H 2B1, Canada; aalgendy@etu.uqac.ca (A.Y.A.); mjavidan@uqac.ca (M.J.); xgchen@uqac.ca (X.-G.C.)
2   Arvida Research and Development Centre, Rio Tinto Aluminum, Saguenay, QC G7S 4K8, Canada; leiray.pan@riotinto.com
*   Correspondence: fyavari@etu.uqac.ca
†   Presented at the 15th International Aluminium Conference, Québec, QC, Canada, 11–13 October 2023.

Abstract: The Aluminum-Nickel alloy system exhibits good potential for rotor applications in electric vehicles, which require good castability, high electrical conductivity (EC), and mechanical strength. In the present study, the microstructure, hot tearing susceptibility (HTS), electrical conductivity, and mechanical properties of binary Al-xNi (x: 1 to 5% wt%) alloys were investigated. The results showed that the Al-1Ni alloy exhibited the highest EC of 57.6% IACS. However, increasing the Ni content to 5% led to a decrease in EC and a significant reduction in HTS. In addition, increasing the Ni content from 1 to 5% slightly enhanced the yield strength from 70.4 to 83.2 MPa showing a weak strengthening effect. The effect of Si and Mg addition on the strength and EC of Al-1Ni alloy was studied. By adding 0.6% Si and 0.6% Mg to the Al-1Ni alloy, the yield strength was enhanced to 156.6 MPa after T5 and 287.5 MPa after T6, respectively, while maintaining a high EC (51% IACS). The significant improvement in yield strength was attributed to the presence of nanosized MgSi precipitates as the strengthening phase, which was confirmed by TEM analysis.

Keywords: Al-Ni alloys; hot tearing susceptibility; electrical conductivity; mechanical strength

1. Introduction

Modern hybrid and electric vehicles in transportation industries require castable alloys that exhibit high electrical conductivity (EC) as well as high strength [1]. Aluminum alloys are desirable materials for these applications due to their low density, high strength-to-weight ratio, and relatively high electrical conductivity [2]. Among the conventional Al cast alloys, those with high strength exhibit poor electrical conductivity (less than 45% IACS), such as A356, and the alloys possessing high EC have low yield strength (less than 100 MPa), such as Castasil 21 [1,3]. Therefore, it is necessary to develop novel Al alloys with a good combination of castability, electrical conductivity, and strength.

Most of conventional Al cast alloys are based on the Al-Si eutectic system because of their excellent casting characteristics, including good fluidity and resistance to hot tearing [4]. Although the addition of Si improves the castability and strength of Al alloys, it is detrimental to the EC [3] due to its relatively high solubility in Al (1.65 wt% in solid solution) [5]. Therefore, an alternative system needs to be designed for castable rotor applications. When adding an alloying element to Al, it can either dissolve into the Al matrix or form precipitates if its concentration exceeds the solubility limit. In the case of a dissolved alloying element, the Al matrix is distorted, interfering with the path of electrons and resulting in a reduction in EC. On the other hand, alloying elements that form precipitates have less impact on the EC since they do not cause as much distortion in the Al lattice as the dissolved elements in the solid solution [5].

Koutsoukis et al. [4] reported that the castability of the Al-Ni system is competitive with Al-Si alloys. The high castability of Al-Ni alloys comes from their short freezing ranges and the high-volume fraction of the eutectic phase [4,6]. In addition, the Al-Ni system exhibits high EC because the maximum solid solubility of Ni in Al is 0.04 wt%, resulting in a high-purity α-Al phase [5]. Due to this low solid solubility, almost all the Ni added to Al forms an Al_3Ni eutectic phase upon solidification of the Al-Ni system [4,5]. Thus, the binary Al-Ni system cannot benefit from solid solution strengthening and precipitation strengthening mechanisms. To improve the mechanical properties of Al-Ni alloys, alloying elements that could provide precipitation strengthening in the Al matrix are desirable. It is a common practice that the addition of Si and Mg is used to improve the mechanical properties of Al alloys due to the formation of Mg_2Si precipitates [7–9]. Many studies revealed that the formation of nanosized Mg_2Si precipitates in the microstructure via an aging heat treatment significantly increased the mechanical properties of the Al alloys [8–10]. Considering the need for high EC, the amount of Si and Mg added to Al-Ni alloys should be kept as low as possible to achieve a good combination of yield strength and EC.

The present study aims to develop a castable Al-Ni based system exhibiting high EC and yield strength. The microstructure, castability, EC, and mechanical properties of Al-xNi binary alloys (x = 1 to 5 wt%) were investigated. Based on the EC results and the cost-effectiveness of the products, Al-1Ni is selected for microalloying with Si and Mg to enhance the simultaneous requirements of both EC and yield strength.

2. Materials and Methods

Five experimental Al-Ni and Al-Ni-Si-Mg alloys were prepared. For each alloy, pure aluminum (99.8%), Al-20%Ni and Al-50%Si master alloys, and pure Mg were melted in a graphite crucible using an electrical resistance furnace. The actual chemical compositions of the studied alloys are given in Table 1. The melt was held at the temperature of 70 ± 5 °C above the liquidus temperature of each alloy and Ar-degassing for 20 min. Once the melt was ready, it was poured into two permanent molds including (1) a steel constrained rod casting (CRC) mold preheated at 250 ± 5 °C for evaluation of hot tearing susceptibility (HTS), and (2) a copper thin-plate mold preheated at 400 ± 5 °C for preparing samples for mechanical testing, EC measurements, and microstructural observation. The dimensions of the cast plates were 100 mm × 80 mm with a thickness of 4 mm. The HTS of binary Al-Ni alloys was predicted by thermodynamic simulation based on the Hu et al. model [11], and the predicted results were compared to the experimental results of CRC samples, which were evaluated based on the method presented in the previous studies [11,12].

Table 1. Chemical compositions of the alloys studied (wt%).

Alloys	Ni	Si	Mg	Fe	Ti	Al
Al-1Ni	1.18	0.05	0.002	0.07	0.03	Bal.
Al-2Ni	2.29	0.08	0.001	0.07	0.02	Bal.
Al-3.5Ni	3.43	0.06	0.001	0.07	0.02	Bal.
Al-5Ni	4.85	0.06	0.001	0.08	0.02	Bal.
Al-1Ni-0.6Si-0.6Mg	1.09	0.63	0.56	0.08	0.03	Bal.

The thin cast plates of Al-1Ni and Al-1Ni-Mg-Si alloys were subjected to T5 and T6 heat treatments. The T6 heat treatment consists of solutionizing at 520 °C for 2 h and aging at 180 °C for 24 h, and for T5 the cast samples were exposed at 180 °C for 24 h. The samples were cut in the cross section for microstructural evaluation using optical microscopy (OM), scanning electron microscopy (SEM), and transaction electron microscopy (TEM). EC was measured using a Sigmascope SMP10 unit with a frequency of 480 kHz based on ASTM E1004. Ten measurements were taken from each sample to obtain the average value of EC in % IACS. Mechanical properties were evaluated by microhardness measurements

and tensile tests. The Vicker hardness test was carried out on at least eight measurements for each sample with a load of 25 g and a dwell time of 20 s, and the average values were reported. The tensile test samples were prepared according to ASTM-E8, and the test was performed at ambient temperature with an extension rate of 0.5 mm/min. The tensile test was repeated three times for each sample.

3. Result and Discussion

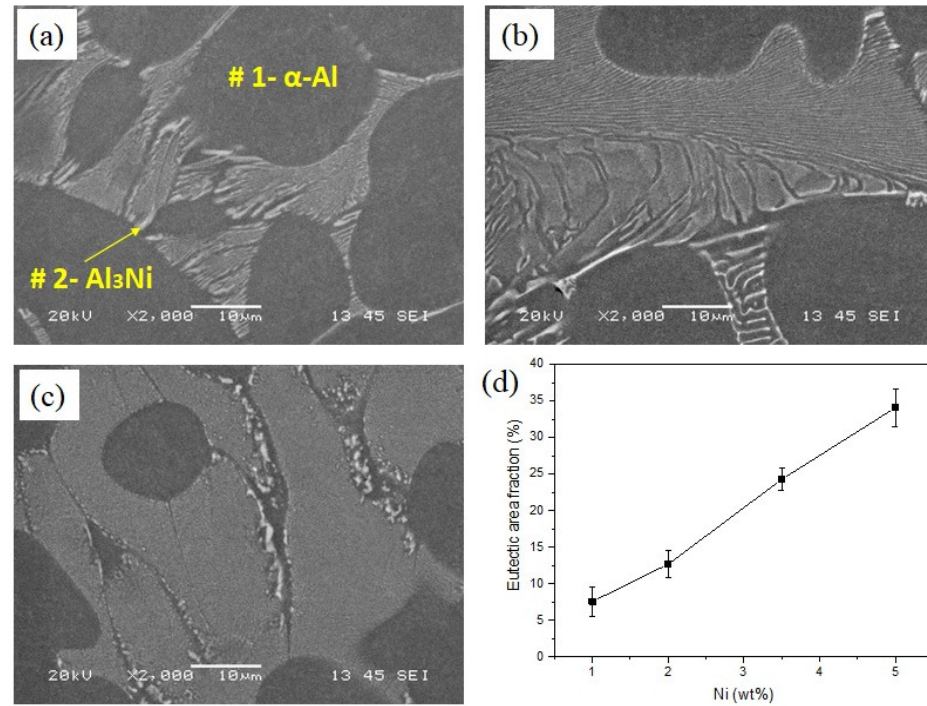### 3.1. Al-Ni Binary Alloys

3.1.1. As-Cast Microstructure

The grain structures of the binary Al-Ni alloys are presented in Figure 1. The grain structures in all four alloys were mainly dendritic equiaxed, which was remarkably refined with increasing Ni content. This has been confirmed with quantitative grain size measurements (Figure 1d). Increasing Ni content from 1 to 5 wt%, results in a considerable decrease in the grain size from 99.3 to 38.6 μm, representing more than 60% reduction. It is reported that the grain size is reversely related to the growth restriction factor (GRF) [13], $mC_0(k-1)$, where k is the distribution coefficient between liquid and solid, m is the slope of the liquid line, and C_0 is the initial composition. According to GRF theory, solutes restrict the growth rate of the growing interface, which allows time for further nucleation to occur [13]. Parameters k and m for Ni in aluminum are 0.007 and −3.3, respectively [13]. GRF for Al-Ni alloys is calculated and presented in Figure 1d. As shown in Figure 1d, by increasing the Ni content from 1 to 5 wt%, GRF increased from 3.28 to 16.4, resulting in a reduction in grain size.
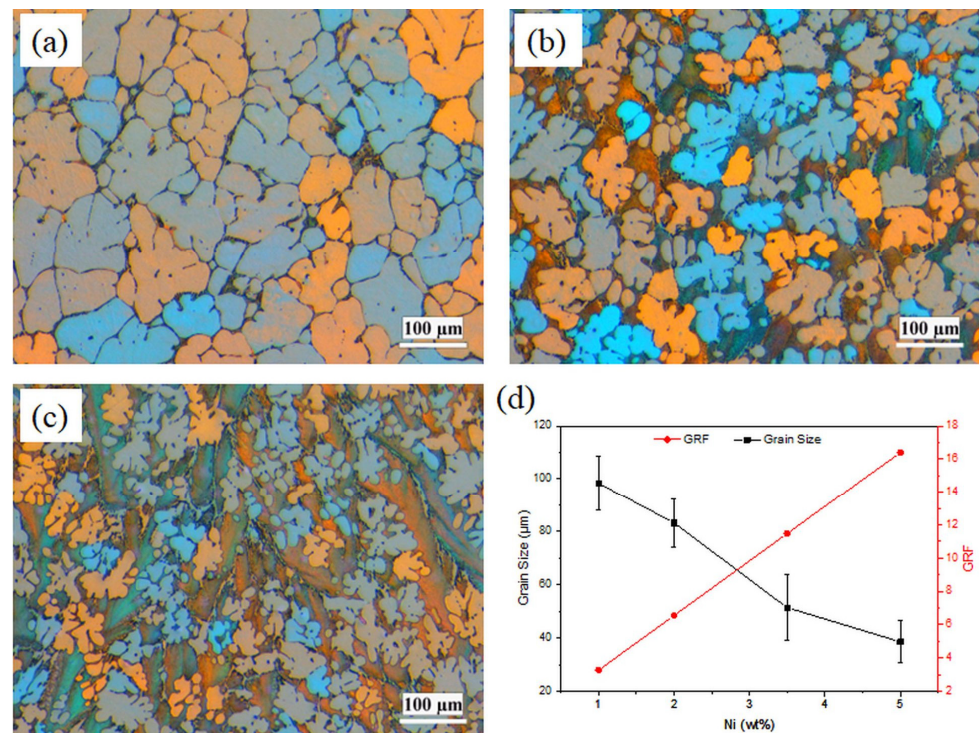
Figure 1. Polarized light optical micrographs showing the grain structure of (**a**) Al-1Ni, (**b**) Al-3.5Ni, (**c**) Al-5Ni, and (**d**) the measured grain size and the growth restriction factor (GRF) as a function of Ni content.

SEM micrographs of the Al-Ni alloys are shown in Figure 2. All the alloys show similar microstructures, featuring primary α-Al dendrites (as the matrix) and eutectic Al-Al$_3$Ni phases. The corresponding EDS analysis of the points in Figure 2a is presented in Table 2. It has been reported that the solid solubility of Ni in Al is negligible [5], as shown in Table 2; this is consistent with our EDS results, which indicated that almost all the added Ni formed

the Al$_3$Ni intermetallics. The area fraction of eutectic Al$_3$Ni intermetallics is calculated by image analysis of optical micrographs and the results are presented in Figure 2d. The area fraction of eutectic Al$_3$Ni increases from 7.6 to 34.8% with increasing Ni content from 1 to 5 wt%.

Figure 2. SEM micrographs (**a**) Al-1Ni, (**b**) Al-3.5Ni, (**c**) Al-5Ni, and (**d**) area fraction of eutectic Al$_3$Ni intermetallics in binary alloys as a function of Ni content.

Table 2. EDS analysis from the points indicated in Figure 2a.

Point	Elements (wt%)	
	Al	Ni
1	100	0
2	71.43	28.57

3.1.2. Hot Tearing Susceptibility (HTS)

Based on the model developed by Hu et al. [11] for the prediction of HTS, the maximum steepness of the plot of T-(f$_S$)$^{1/3}$, for an equiaxed grain structure can be considered as an index for the hot tearing susceptibility, where T is temperature and f$_S$ is the fraction of solid. As the slope of dT/d(f$_S$)$^{1/3}$ is negative, the absolute value of the slope is considered the HTS index [11]. For the prediction of HTS, the maximum slope of the curves |dT/d(f$_S$)$^{1/3}$| just before the eutectic reaction is calculated.

T vs. (f$_S$)$^{1/3}$ plots for four Al-Ni alloys are presented in Figure 3a. The predicted results are presented in Figure 3b and compared with the experimental results. Both experimental and predicted results show that by increasing Ni content, the hot tearing susceptibility of Al-Ni alloys reduced. There are many factors affecting the HTS of an alloy, including freezing range [11], grain refinement [14,15], and eutectic fraction [11]. Generally, hot tearing resistance increases with increasing eutectic liquid fraction [11] and decreasing grain size [16]. In this study, the decrease of the HTS with Ni addition could be explained by the grain size reduction (as shown in Figure 1) and the increase in the area fraction of the Al$_3$Ni eutectic phase (Figure 2). Grain refinement reduces the hot tearing sensitivity of alloys because it delays the grain coherency point and consequently improves the feeding

ability of the remaining melt [16]. In addition, increasing the volume fraction of the eutectic phases can reduce the HTS by refilling the initially formed tears.
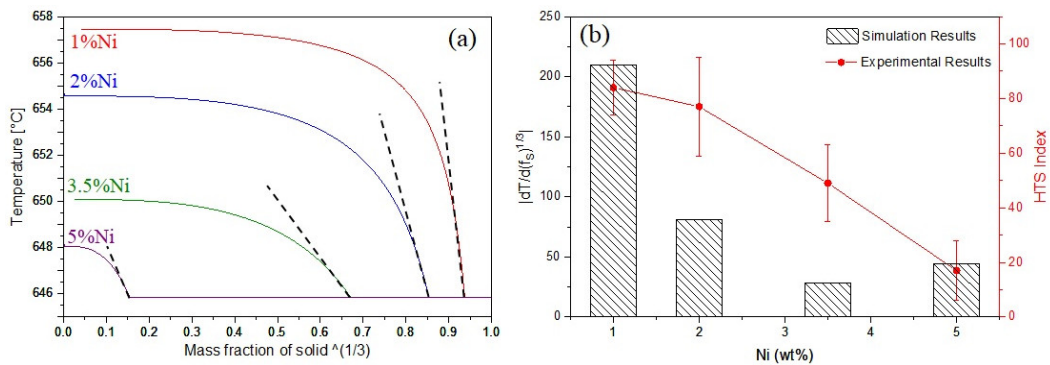

Figure 3. (**a**) T vs. $(f_S)^{1/3}$ plots; (**b**) measured and simulated hot tearing susceptibility.

3.1.3. Electrical Conductivity and Mechanical Properties

The measured EC, yield strength (YS), and microhardness (HV) of Al-Ni alloys are presented in Figure 4. With increasing Ni content, the EC decreased from 57.6% IACS in Al-1Ni to 52.8% IACS in Al-5Ni. Comparing these results with the literature, the effect of Ni addition on the EC of Al alloys is far less destructive than Si addition [3,17]. According to Mulazimoglu et al. [17] the addition of 2 wt% Si to Al decreased the EC of Al to less than 50% IACS. The better EC of Al-Ni based alloys can be associated with the lower solid solubility of Ni in Al (0.04 wt% at eutectic temperature) compared to Si (1.65 wt% at eutectic temperature) [5]. EDS analysis of the α-Al phase (Table 2) indicates that the solid solubility of Ni in Al is negligible. Increasing Ni from 1 to 5 wt% decreased the EC of Al-Ni alloys by 8%, which is attributed to the increasing supersaturation level of Ni in the Al matrix and the increasing proportion of the Al_3Ni intermetallic phase (Figure 2d).
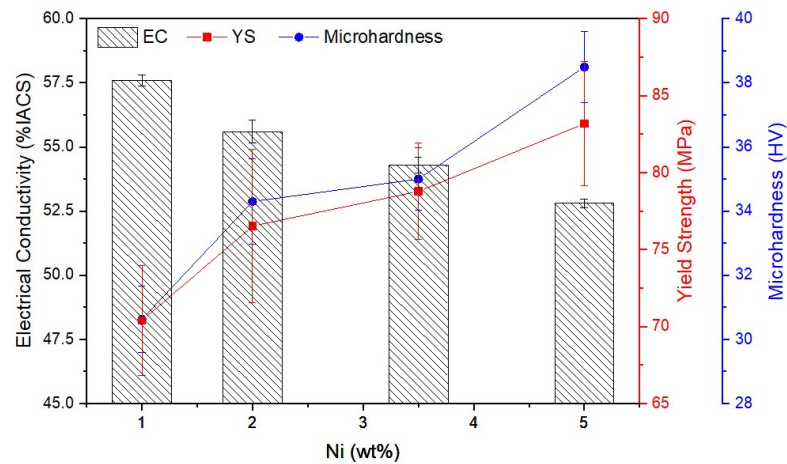

Figure 4. Electrical conductivity, yield strength, and microhardness of Al-Ni alloys as a function of Ni content.

According to Figure 4, with increasing Ni addition up to 5 wt%, the microhardness of samples moderately increased from 30.6 to 38.5 HV, and the YS increased from 70.4 to 83.2 MPa as a result of the increase in the area fraction of eutectic Al_3Ni intermetallics. According to Sankanit et al. [18], the Al_3Ni intermetallic phase is noticeably harder than the Al matrix. Therefore, increasing the amount of eutectic Al_3Ni intermetallics in Al-Ni alloys improves the mechanical strengths (hardness and YS) attributed to the strengthening effect of the Al_3Ni intermetallic phase [18].

3.2. Microalloying with Si and Mg

Developing high-performance Al-based castable rotor products is challenging; this becomes even more difficult when taking into account the mutually exclusive properties of EC, mechanical strength and castability at the same time. Among the four binary Al-Ni alloys studied, Al-1Ni exhibited the best EC, with an experimental HTS value comparable to Al-2Ni (Figure 3b). In addition to the higher EC, because of the high cost of Ni, it was decided to keep Ni content as low as possible. Although the addition of Ni up to 5 wt% improved the mechanical strength, the strengthening of eutectic Al_3Ni intermetallics was far too weak (Figure 4). To significantly improve the strength of rotor products, it is necessary to introduce highly efficient precipitates as the strengthening phase. In this study, the Al-1Ni alloy was selected to investigate the microalloying effect with Si and Mg on strength and EC.

3.2.1. Microstructure of Al-1Ni-0.6Si-0.6Mg

The microstructure of the Al-1Ni-0.6Si-0.6Mg alloy in as-cast and solution-treated conditions is shown in Figure 5. The SEM-EDS analysis was conducted to identify the different phases observed in Figure 5a, and the results are presented in Table 3. In the as-cast condition, the microstructure of the Al-1Ni-0.6Si-0.6Mg alloy consists of a network of irregular shaped Al_3Ni intermetallics (marked as #1) and primary Mg_2Si phase (marked as #3), distributed in the interdendritic region. In addition, a small amount of round Al(SiMgNi) ternary eutectic phase was mainly distributed in the α-Al matrix (marked as #2). After solution heat treatment, the Al(SiMgNi/Fe) ternary eutectic phase was completely dissolved, and little Mg_2Si was occasionally detected. In contrast, no remarkable change in the Al_3Ni intermetallics was observed.
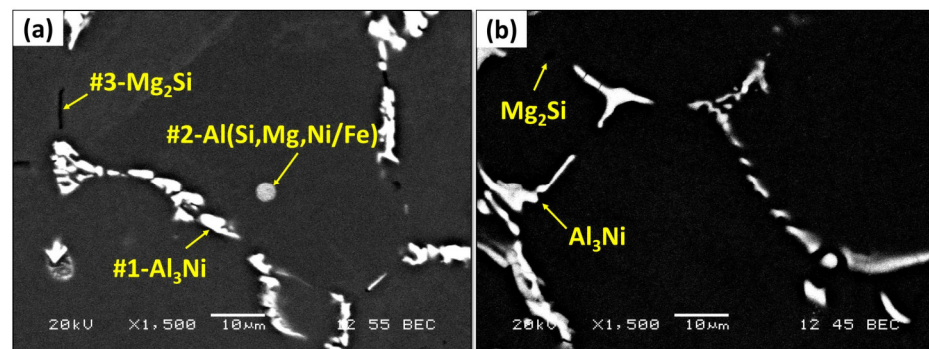

Figure 5. The microstructure of Al-1Ni-0.6Si-0.6Mg (**a**) as-cast and (**b**) solution-treated conditions.

Table 3. EDS analysis from the points indicated in Figure 5a.

Location	Phase Type	Elements, wt%			
		Ni	Si	Mg	Al
Point 1	Al_3Ni	29.30	-	-	70.70
Point 2	Al(SiMgNi/Fe)	10.10	17.90	6.26	65.74
Point 3	Mg_2Si	-	37.35	62.65	-

Figure 6 displays the typical bright-field TEM images showing the evolution of nano-sized Mg/Si precipitates after T5 and T6 heat treatment. All TEM images were taken along the $[001]_{Al}$ zone axis. As shown in Figure 6a, the precipitates after T5 temper are fine (41.9 nm in length and 4.03 ± 0.15 nm^2 cross-sectional area), which is believed to be β''. On the other hand, the precipitates after T6 temper are slightly larger than those in the T5-temper. According to the precipitate size, there is a mixture of β'' and β', but the major strengthening phase is β''. The T6 samples underwent the high-temperature solution treatment (520 °C for 2 h) before aging, which leads to more Si and Mg solute

atoms dissolved in the Al matrix. Therefore, during aging there are more solute atoms to be extracted from the matrix to form a high number density of MgSi precipitates.
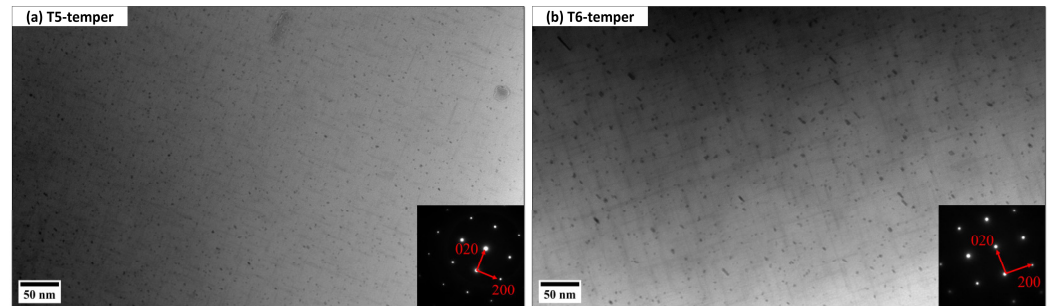
Figure 6. Typical bright-field TEM images showing the precipitation of nanosized MgSi (**a**) β'' after T5 and (**b**) a mixture of β'' and β' after T6.

3.2.2. Electrical Conductivity and Mechanical Properties

The EC and YS of Al-1Ni and Al-1Ni-0.6Si-0.6Mg alloys are presented in Figure 7 and compared with other alloys from the literature [1]. By adding Si and Mg to Al-1Ni, the electrical conductivity decreased from 57.6 to 48.5% IACS in the as-cast condition. The lower electrical conductivity could be explained by the presence of Si and Mg solute atoms in the Al, which has a detrimental effect on scattering electrons. After the T5 and T6 heat treatments, electrical conductivity increased to 51% IACS, since the precipitation of MgSi particles after aging removes Si and Mg solute atoms from the α-Al matrix.
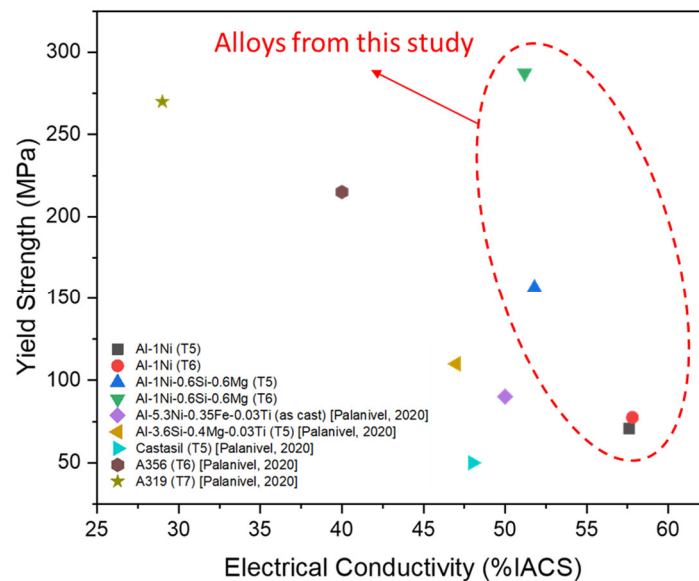
Figure 7. Electrical conductivity and yield strength of Al-1Ni and Al-1Ni-0.6Si-0.6Mg alloys compared with other alloys from the literature [1].

The tensile results indicated that the binary Al-1Ni alloys are not heat-treatable and their YS remained at a low level (~75 MPa after T5 and T6). However, Al-1Ni-0.6Si-0.6Mg after T5 and T6 exhibited a YS of 156.6 and 287.5 MPa, respectively, much higher than the binary Al-1Ni alloy. The formation of a high number density of nanosized MgSi precipitates after aging is the main cause for the improvement of mechanical properties of Al-1Ni-0.6Si-0.6Mg. This alloy with EC of 51% IACS and YS of 157–287 MPa in both T5 and T6 conditions, can well fulfill the targeted specification for electric rotor applications. According to the results in Figure 7, the designed alloy in T5 condition already exhibited a good combination of EC and strength relative to other Al-Si and Al-Ni-based alloys reported in the literature.

When treated in T6 temper, the YS of this alloy was significantly enhanced and even higher than conventional cast Al-Si alloys (A356 and A319), while maintaining excellent EC.

4. Conclusions

The microstructure, electrical conductivity, mechanical properties, and castability of Al-xNi (x = 1 to 5 wt%) and Al-1Ni-0.6Si-0.6Mg alloys were investigated. The Al-1Ni presented the highest EC of 57.6% IACS; by increasing Ni content to 5%, the EC was reduced to 52.8% IACS, whereas the HTS index decreased from 84 in Al-1Ni to 17 in Al-5Ni. By increasing Ni content from 1 to 5%, the yield strength only slightly increased from 70.4 to 83.2 MPa. The Al-Ni binary alloys suffered from low mechanical strength, due to the lack of solid solution hardening and precipitation strengthening in the Al matrix. Therefore, the impact of microalloying with Si and Mg in the Al-1Ni alloy on strength and EC was explored. The Al-1Ni-0.6Si-0.6Mg alloy exhibited a YS of 156.6 MPa and 287.5 MPa after T5 and T6 tempers, respectively, while maintaining a high EC of 51% IACS. Thus, the newly developed Al-1Ni-0.6Si-0.6Mg alloy exhibited an excellent combination of EC and yield strength, which can well fulfil the targeted specification for electric rotor applications.

References

1. Palanivel, S. Aluminum Alloys for Die Casting. International Patent WO 2020/028730 A1, 2 February 2020.
2. Li, Y.; Hu, A.; Fu, Y.; Liu, S.; Shen, W.; Hu, H.; Nie, X. Al Alloys and Casting Processes for Induction Motor Applications in Battery-Powered Electric Vehicles: A Review. *Metals* **2022**, *12*, 216. [CrossRef]
3. Palanivel, S. Casting Aluminum Alloys for High Performance Application. U.S. Patent No. 2019/0127824 A1, 2 May 2019.
4. Koutsoukis, T.; Makhlouf, M.M. Alternatives to the Al–Si Eutectic System in Aluminum Casting Alloys. *Int. J. Met.* **2016**, *10*, 342–347. [CrossRef]
5. Kotiadis, S.; Zimmer, A.; Elsayed, A.; Vandersluis, E.; Ravindran, C. High Electrical and Thermal Conductivity Cast Al-Fe-Mg-Si Alloys with Ni Additions. *Metall. Mater. Trans. A* **2020**, *51*, 4195–4214. [CrossRef]
6. Yang, L.; Li, W.; Du, J.; Wang, K.; Tang, P. Effect of Si and Ni contents on the fluidity of Al-Ni-Si alloys evaluated by using thermal analysis. *Thermochim. Acta* **2016**, *645*, 7–15. [CrossRef]
7. Zhu, M.; Jian, Z.; Yang, G.; Zhou, Y. Effects of T6 heat treatment on the microstructure, tensile properties, and fracture behavior of the modified A356 alloys. *Mater. Des.* **2012**, *36*, 243–249. [CrossRef]
8. Yıldırım, M.; Özyürek, D. The effects of Mg amount on the microstructure and mechanical properties of Al–Si–Mg alloys. *Mater. Des.* **2013**, *51*, 767–774. [CrossRef]
9. Estey, C.; Cockcroft, S.; Maijer, D.; Hermesmann, C. Constitutive behaviour of A356 during the quenching operation. *Mater. Sci. Eng. A* **2004**, *383*, 245–251. [CrossRef]

10. Thirugnanam, A.; Sukumaran, K.; Pillai, U.T.; Raghukandan, K.; Pai, B.C. Effect of Mg on the fracture characteristics of cast Al–7Si–Mg alloys. *Mater. Sci. Eng. A* **2007**, *445–446*, 405–414. [CrossRef]

11. Hu, B.; Li, Z.; Li, D.; Ying, T.; Zeng, X.; Ding, W. A hot tearing criterion based on solidification microstructure in cast alloys. *J. Mater. Sci. Technol.* **2022**, *105*, 68–80. [CrossRef]

12. Razaz, G.; Carlberg, T. Hot Tearing Susceptibility of AA3000 Aluminum Alloy Containing Cu, Ti, and Zr. *Metall. Mater. Trans. A* **2019**, *50*, 3842–3854. [CrossRef]

13. Easton, M.; StJohn, D. Grain Refinement of Aluminum Alloys: Part I. The Nucleant and Solute Paradigms—A Review of the Literature. *Metall. Mater. Trans. A* **1991**, *30*, 1613–1623. [CrossRef]

14. Hao, D.; Fu, H.; Liu, Z.; Chen, R.; Zhong, Z.; Tang, D. Compensation of solidification contraction and hot cracking tendency of alloys. *Acta Metall. Sin.* **1997**, *33*, 921–926.

15. Dahle, A.K.; Tøndel, P.A.; Paradies, C.J.; Arnberg, L. Effect of grain refinement on the fluidity of two commercial Al-Si foundry alloys. *Metall. Mater. Trans. A* **1996**, *27*, 2305–2313. [CrossRef]

16. Liao, H.C.; Liu, Y.; Lü, C.L.; Wang, Q.G. Effect of Ce addition on castability, mechanical properties and electric conductivity of Al–0.3Si–0.2Mg alloy. *Int. J. Cast Met. Res.* **2015**, *28*, 213–220. [CrossRef]

17. Mulazimoglu, M.H.; Drew, R.A.; Gruzleski, J.E. The electrical conductivity of cast Al− Si alloys in the range 2 to 12.6 wt pct silicon. *Metall. Trans. A* **1989**, *20*, 7. [CrossRef]

18. Sankanit, P.; Uthaisangsuk, V.; Pandee, P. Tensile properties of hypoeutectic Al-Ni alloys: Experiments and FE simulations. *J. Alloys Compd.* **2021**, *889*, 161664. [CrossRef]